High-resolution angle-resolved photoemission studies of the surface states on Al(111) and Al(001)

S. D. Kevan, N. G. Stoffel, and N. V. Smith
AT&T Bell Laboratories, Murray Hill, New Jersey 07974
(Received 16 May 1984)

High-resolution angle-resolved photoemission has been used to study Al(111) and Al(001). Two new surface states at $\bar{\Gamma}$ and $\bar{K}$ of Al(111) were observed and characterized. Their energy positions are in good accord with recent self-consistent calculations. The state at $\bar{\Gamma}$ is observed over a narrow range of photon energies near $h\nu = 53$ eV. A simple model is presented which explains this observation and gives a rough estimate of the decay length of the surface state into the bulk. Further studies of the evolution of the peak width as a function of parallel momentum for the $\bar{\Gamma}$ surface state on both surfaces indicates the presence of a new broadening mechanism. Interactions of the initial and final states with the nearby bulk continuum is suggested.

I. INTRODUCTION

Owing to its simple, nearly-free-electron (NFE) nature, aluminum has served as a model for calculations of surface electronic structure. In 1971 Boudreaux, performed calculations in which he predicted surface states on the (001) and (111) surfaces located in projected gaps in the bulk band structure opened by the weak lattice potential at the Brillouin-zone boundaries.[1] He was able to describe the energies of these states, as well as characterize their wave functions by their decay length into the bulk of the crystal. Angle-resolved photoemission spectroscopy (ARPES) experiments have since detected various surface states and resonances on aluminum crystals.[2–5] The dispersion relations measured in these experiments are generally in good agreement with recent, more sophisticated self-consistent calculations.[6–9]

The experimental situation, however, is not complete. In particular, several calculations predict surface states on Al(111) at the $\bar{\Gamma}$- and $\bar{K}$-symmetry points of the surface Brillouin zone which have not yet been detected.[1,6–8] In addition, ARPES experiments have the ability to measure more than just dispersion relations. Measurements of the intensity of a surface state as a function of photon energy have been shown, using a tight-binding treatment,[10] to yield information on the state's wave function. We describe here a simple model for NFE systems, and apply it to a newly observed surface state at $\bar{\Gamma}$ on Al(111). Moreover, high-resolution ARPES experiments can be applied to measure the observed peak width as a function of binding energy or parallel momentum. Recent experiments on copper surface states have isolated at least two independent broadening mechanisms:[11–13] photohole lifetime broadening and parallel-momentum broadening caused by surface defects and impurities. A similar analysis in the case of the surface states dispersing parabolically about $\bar{\Gamma}$ on Al(001) and Al(111) shows that the broadening cannot be completely explained by these two mechanisms, providing definitive evidence for the existence of an additional mechanism.

The structure of this paper is as follows: The experimental procedures are described in the next section. Results concerning the existence, dispersion, and photon-energy dependence of two Al(111) surface states are described and analyzed in Sec. III. In Sec. IV we elaborate on the widths of the surface states at $\bar{\Gamma}$ on Al(001) and Al(111). The final section summarizes our conclusions.

II. EXPERIMENTAL PROCEDURES

High-purity (99.999%) aluminum crystals were cut and polished normal to the [111] and [001] axes to within 0.5°. These were chemically etched and inserted into the vacuum system, and cleaned by several ion-bombardment—annealing cycles [1000-eV Ne^+ ions, $\sim 5\mu A/cm^2$, $\sim$30-min sputter; 400 °C, (5—10)-min anneal]. This treatment produced atomically clean surfaces with good crystalline quality as determined by low-energy electron-diffraction and Auger-electron spectroscopy. The ARPES experiments were performed using a spectrometer described elsewhere.[14] Experiments on Al(001) utilized Ar I resonance radiation ($\hbar\omega = 11.8$ eV), while those on Al(111) were performed at the National Synchrotron Light Source at Brookhaven National Laboratory. A 6-m toroidal-grating monochromator provided photons between 10 and 100 eV in these experiments, with a resolution of better than 100 meV.[15]

III. SURFACE STATES ON Al(111)

A. Results near $\bar{\Gamma}$

While ARPES has been used to observe surface states on numerous single-crystal metal surfaces,[16,17] it is useful to review its application in this respect. True surface states exist in band gaps of the three-dimensional band structure projected onto the two-dimensional Brillouin zone.[18] Ideally, to verify the assignment of a surface state, an experiment will delineate the key features of this projected gap and show that the surface state exists in the gap. In addition, a surface state must not disperse with the component of momentum normal to the surface, and

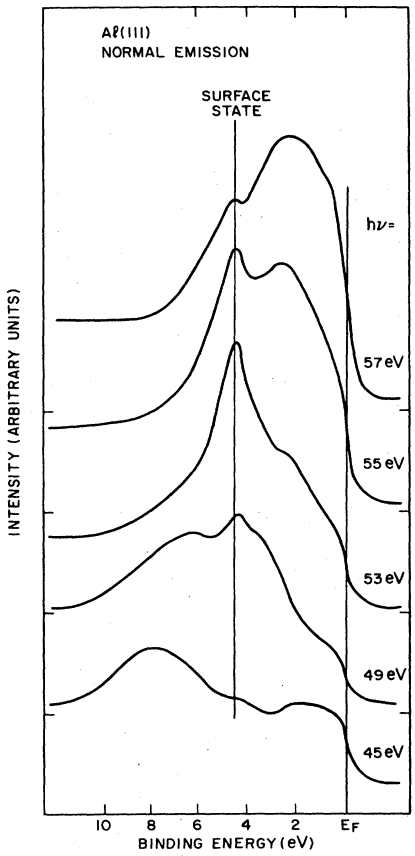

FIG. 1. ARPES energy-distribution curves collected at normal emission from Al(111) in the region near $k_\perp = 1.34$ Å^{-1}. The surface state is observed as a nondispersive peak at $E_B \sim 4.6$ eV, while the broader features arise from bulk transitions.

its parallel dispersion must show the symmetry of the surface rather than that of the bulk. A further test involves enhanced sensitivity to contamination for a surface state relative to a bulk state.[16] Finally, a test which has recently become popular involves measuring the surface-state intensity as a function of final-state momentum normal to the surface.[10] A surface state will show intensity oscillations centered on the symmetry points of the bulk zone. None of these tests is by itself definitive; a combination of several provides compelling evidence for a surface-state identification.

Figure 1 shows normal-emission energy-distribution curves (EDC's) on Al(111) for $45 \leq h\nu \leq 57$ eV. In the direct-transition model, the final-state momentum normal to the surface is given by[4,19,20]

$$k_\perp = \left[\frac{2m^*}{\hbar^2}(h\nu - E_B - V_0) \right]^{1/2} . \quad (1)$$

For this range of photon energies, the EDC's sample initial states along Λ near the L point of the bulk band structure. The L point corresponds most closely to $h\nu = 53$ eV. Two free-electron initial-state bands which cross at L are split by the lattice-potential matrix element $V_{111} = -0.21$ eV.[21] These two bands can be seen as broad, dispersing peaks in Fig. 1. The lower band is more intense before L, while the upper (umklapp) band is more intense above L. This transfer of intensity from the lower to upper bands was observed on Al(001) (Ref. 4) as well, albeit to a lesser degree, and can be understood using an approximate, one-dimensional treatment. The lower and upper initial-state bands are written as

$$\psi_\pm = A_\pm e^{i\mathbf{k}\cdot\mathbf{x}} + B_\pm e^{i(\mathbf{k}-\mathbf{G}_1)\cdot\mathbf{x}} .$$

In the present case, $\mathbf{G}_1$ corresponds to the bulk reciprocal-lattice vector (1,1,1) $(2\pi/a)$. The final state can be taken as a single plane wave,

$$\psi_f = e^{i(\mathbf{k}+\mathbf{G}_2)\cdot\mathbf{x}} ,$$

where $\mathbf{G}_2$ corresponds to (3,3,3) $(2\pi/a)$. If we estimate the photoemission intensity in each band by

$$I_\pm \sim |\langle \psi_f | \nabla V | \psi_\pm \rangle|^2 ,$$

and expand V in terms of lattice-potential matrix elements

$$V(\mathbf{r}) = V_0 + \sum_{\mathbf{G}} V_{\mathbf{G}} e^{i\mathbf{G}\cdot\mathbf{r}} ,$$

then eventually we obtain

$$I_\pm \sim |A_\pm \mathbf{G}_2 V_{\mathbf{G}_2} + B_\pm (\mathbf{G}_2 - \mathbf{G}_1) V_{\mathbf{G}_2 - \mathbf{G}_1}|^2 .$$

The coefficients $B_\pm$ change sign when $\mathbf{k}$ is swept through $\mathbf{G}_1/2$, so that on one side of the symmetry point (L in our case) the two terms add for one band and tend to cancel for the other, while the opposite is true for the other side of the symmetry point. Thus the intensity will appear to transfer from one band to the other at the symmetry point. The sharpness of this transfer depends, in part, on how quickly the coefficients $A_\pm$ and $B_\pm$ change in magnitude, which, in turn, depends on $V_{\mathbf{G}_1}$. This explains qualitatively why the intensity switch is more pronounced on Al(111) than on Al(001).

A third, sharper and nondispersive peak appears in Fig. 1 at $E_B = (4.56 \pm 0.04)$ eV relative to the Fermi energy. This peak dominates the spectrum over a narrow energy range near $h\nu \sim 53$ eV. Since there is no nondispersive band for this line in $\mathbf{k}$ space, this peak must be either an umklapp peak,[16,19] a density-of-states feature, a surface-state, or a surface resonance. The former is easily ruled out since no such peak could be nondispersive in this case. The gap at L introduces two density-of-states singularities separated by $\sim 2V_{111}$. Considering the discussion of the preceding paragraph, one would expect to sample predominantly the lower singularity for $h\nu \leq 53$ eV and the higher one for $h\nu \geq 53$ eV, implying that the energy position of such a density-of-states feature would be expected to change with photon energy. Such behavior is not observed. In addition, while the peak is not completely quenched by surface contaminants, it is more sensitive than the neighboring bulk transitions. The opposite behavior would be expected for a density-of-states feature. While we cannot rule out small contributions from density-of-states features, the most consistent assignment is as a surface state or surface resonance. The peak is lo-

cated in a projected gap of the *calculated* band structure,[7,8,21] implying that it is a true surface state. However, the large inherent widths of the peaks involved, compared to the width of the gap, do not allow an accurate experimental measurement of the limits of the bulk continuum, so that the distinction between a surface state and a surface resonance is not rigorous. We prefer to call it a surface state, and will return to this point shortly. We note that a similar state located in the gap at L projected onto the $\bar{X}$ point of Al(001) has recently been observed.[4] In addition, a recent self-consistent linear combination of Gaussian orbitals calculation for the Al(111) surface predicts a slowly decaying surface state located in the projected gap at $\bar{\Gamma}$ at a binding energy of 4.68 eV, in good accord with our results.[8] A different self-consistent calculation[7] fails to discern this state, but the criterion they used to identify a true surface state is more stringent, and the long decay length of this state (see below) might have prevented its assignment as a surface state.

Before proceeding to analyze the photon-energy dependence of the surface-state intensity, it is useful to describe its dispersion parallel to the surface. Figure 2 shows EDC's of the surface state as a function of emission angle

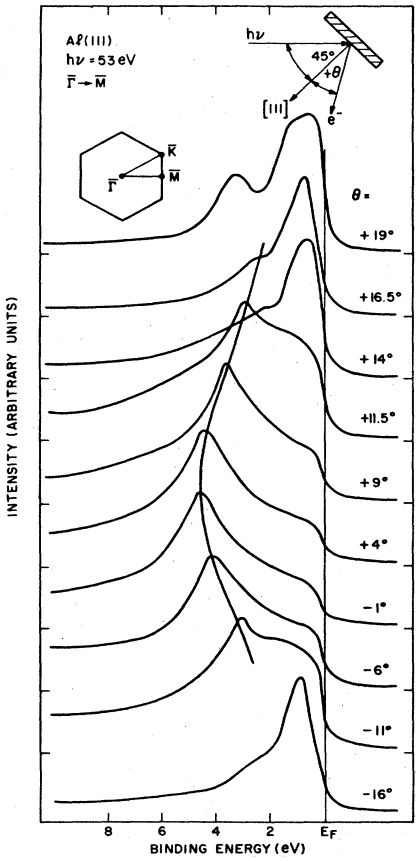

FIG. 2. ARPES energy-distribution curves of Al(111) at $h\nu=53$ eV at various polar emission angles in the $\bar{\Gamma}\rightarrow\bar{M}$ azimuth. Note the upward dispersion of the surface state about normal emission and the eventual merging with a bulk feature near $\theta=\pm 15°$.

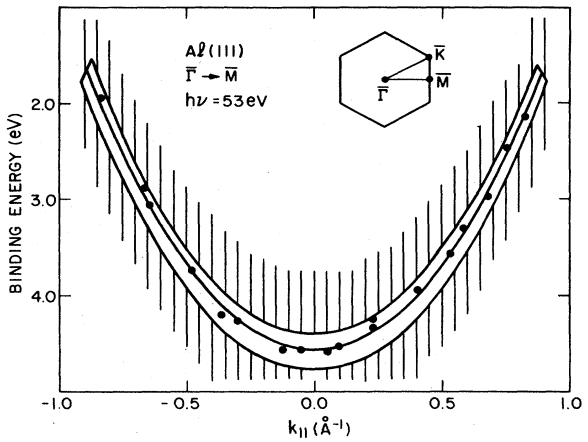

FIG. 3. Experimental dispersion relation for the $\bar{\Gamma}$ surface state on Al(111), showing a parabolic fit with an effective mass $m^*=(1.03\pm0.01)m_e$. Hatched region is the calculated bulk continuum.

or, equivalently, parallel momentum, for $h\nu=53$ eV. Near $k_{\parallel}=0.9$ Å^{-1}, the surface-state peak merges with a bulk transition and becomes indistinguishable. The dispersion relation derived from these data is shown in Fig. 3, superimposed on the projection of the calculated bulk continuum onto the two-dimensional Brillouin zone. The effective mass of the dispersion relation is fitted to be $m^*=1.03m_e$, compared to $1.18m_e$ measured for the $\bar{\Gamma}$ surface state on Al(001).[2–4] As mentioned before, the surface state remains in the projected gap until it crosses into the bulk continuum near the value of $k_{\parallel}$, where it merges with a bulk feature in Fig. 2. Unfortunately, the proximity of this bulk transition makes an accurate study of this crossing prohibitively difficult.[22] The results in the final section indicate that, most likely, no dramatic effect would be observed in any case.

B. Discussion

As mentioned earlier, the surface state is observable over a narrow range of final-state momenta near the L point. The reason for this is related to the fact that this state decays rather slowly into the bulk. We show below that the sharpness of the surface-state intensity is related to its definition in frequency space. A long decay length results in a sharp frequency spectrum and visibility over a narrow photon-energy range.

Such oscillations are well documented for Cu(111),[10] Al(001),[4] Cu(001),[23] and Au(111).[23] The accepted explanation for this phenomenon is reviewed as follows.[10] The surface-state wave function ψ_s is expanded in terms of bulk wave functions ψ_B at the same $k_{\parallel}$:

$$\psi_s=\sum_{k_\perp}\alpha_{n,k\perp}\psi_B^n(k_\perp)\,. \tag{2}$$

The sum is over all $k_\perp$ and all n bands of the bulk band structure. The surface-state intensity is given by Fermi's golden rule:

$$I\sim|\langle\psi_s|\mathbf{A}\cdot\mathbf{p}|\psi_f\rangle|^2$$
$$\sim|\langle\textstyle\sum\alpha_{k\perp}\psi_B^n(k_\perp)|\mathbf{A}\cdot\mathbf{p}|\psi_f\rangle|^2\,. \tag{3}$$

The direct-transition model implies that, for a particular final state $\psi_f(k_\perp)$, determined by the final-state energy and momentum, only a particular term in the sum over $k_\perp$ [given by Eq. (1)] will contribute appreciably. In addition, usually only contributions from one bulk band n' need be considered, and the bulk matrix element may be taken as constant over a small range of final-state momenta. We obtain, as before,[10]

$$I_s \propto |\alpha_{k\perp,n'}|^2 . \tag{4}$$

The coefficients $\alpha_{k\perp}$ are normally peaked around the particular value of $k_\perp$ where the bulk band is closest in energy to the surface state. In the present case, this occurs at the L point, and the dominant oscillation frequency of the surface-state wave function normal to the surface corresponds to that of the lower bulk band at L. The surface-state intensity is predicted and observed to peak when $k_\perp$, in the extended-zone scheme, is near an L point. The experimental situation is complicated by the fact that the total spectral intensity is transferred between surface-state and bulk peaks.[4,24,25] This is observed in Fig. 1: Near $h\nu=53$ eV, the two bulk peaks contribute little compared to the dominant surface-state peak. This has been explained in the case of copper.[24] In addition, the observed bulk dispersion relation is perturbed relative to the real relation by the proximity of the surface state.[24,25]

In order to analyze these results quantitatively, we performed a three-peak fit to the EDC's in Fig. 1. We used simple Lorentzian line shapes folded with a Fermi function, and assumed a cubic polynomial background. The unusual line shapes evident in the figure introduce errors in this procedure which we estimate to be less than 10%. We then compared the surface-state intensity I_s to the total valence-band intensity, $I_{\rm tot}=I_s+I_{B1}+I_{B2}$, where I_{B1} and I_{B2} are the intensities of the two bulk peaks. In Fig. 4 we plot $I_s/I_{\rm tot}$ as a function of $k_\perp$ derived from Eq. (1) and normalized to $k_L=1.34$ Å^{-1}. There are likely some systematic errors in this fitting procedure, since there is significant overlap of the peaks. As evidenced by inspection of Fig. 1, however, the general shape and full width at half maximum of the curve in Fig. 4 is readily discernable in the spectra, and the peak at $k_\perp/k_L=3$ is real. A qualitatively similar curve was published earlier for Al(001).[4] In that case, however, the curve is split at its maximum and is 3—4 times broader. No splitting was observed on Al(111). In addition, the Al(001) data show a secondary structure which was ascribed to interference effects from different X points. No interference is possible in the present case since the sharpness of the peak precludes any overlap in momentum space of neighboring resonances. The theoretical curves in Fig. 4 are the result of the simple NFE model detailed below.

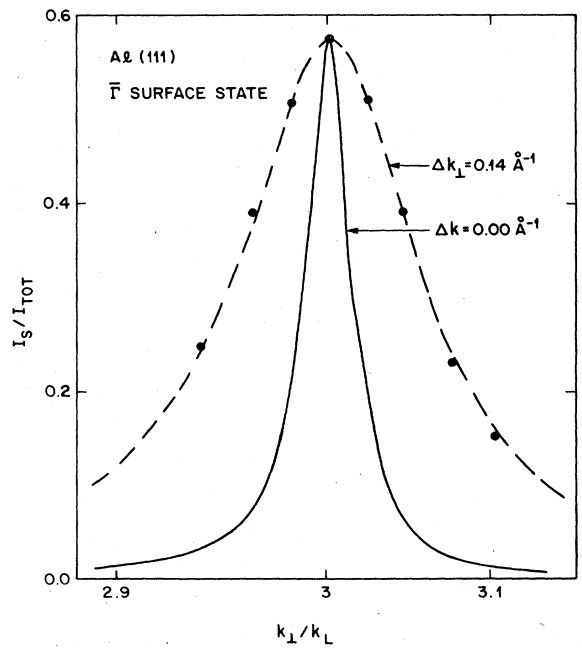

FIG. 4. Surface-state intensity relative to the total valence-band intensity as a function of final-state momentum normal to the surface. Points are the experimental results extracted from Fig. 1, while the solid and dashed curves are the unbroadened and perpendicular-momentum-broadened results from a simple model, respectively (see text). The curves are normalized to have the same maximum intensity as the experimental points.

C. NFE model for surface-state intensity

Our model is similar in spirit to that used to treat oscillations in copper surface-state intensities,[10] but is based on a NFE rather than a tight-binding model. We start by reducing the problem to one dimension without losing any generality. This reduction relies on the bulk band contours near L depending mostly on V_{111}, and the parallel dispersion being well behaved (i.e., parabolic). Both of these are good approximations in this case. Our goal is to approximate Eq. (2), and then to use Eq. (4) to calculate I_s. For $\psi_B(k)$, we use a NFE wave function,

$$\psi_B(k)=C_1 e^{ikx}+C_2 e^{i(k+g)x} .$$

The constants C_1 and C_2 are determined by solving the simple secular equation, with off-diagonal elements given by V_{111}, the inner potential $V_{000}=-11.6$ eV, and the reciprocal-lattice vector g appropriate for the L point. We then have

$$\alpha_{k_\perp}=C_1\langle k\,|\,\psi_s\rangle+C_2\langle k+g\,|\,\psi_s\rangle , \tag{5}$$

which clearly shows how we sample the frequency spectrum of the surface-state wave function. A physically reasonable, yet analytical, form for ψ_s has been derived in the NFE case.[26,27]

$$\psi_s(x)=\begin{cases} N e^{qx}\cos(k_L x+\delta), & x<0 \\ N\cos(\delta)e^{-V_0 qx/V_1}, & x>0 \end{cases} \tag{6}$$

where $x=0$ is the surface plane and the bulk extends in the $-x$ direction. The values of the various parameters are given as follows:

$$V_0 = -V_{000} > 0, \quad V_1 = -V_{111} > 0 ,$$

$$q \equiv 1/\lambda_i = \frac{V_1}{V_0 + V_1}[K^2(V_0 + V_1) - k_L^2]^{1/2} , \tag{7}$$

$$\delta = \cos^{-1}\left\{\frac{k_L}{[K^2(V_0 + V_1)]^{1/2}}\right\}, \quad 0 \le \delta \le \pi/2 \tag{8}$$

$$K^2 = 2m/\hbar^2 = 0.262 \text{ Å}^{-2} \text{ eV}^{-1} .$$

N is the normalization constant.[27] There are three features which make this function reasonable for our purposes. First, the function decays exponentially outside the surface, with decay length

$$\lambda_o = (V_1/V_0)\lambda_i . \tag{9}$$

This is the correct limiting form. Second, the function oscillates inside the bulk at the frequency of the symmetry point, k_L.[26] The phase shift δ is required for matching at $x = 0$.[26,27] Finally, the function decays into the bulk with a decay length given by λ_i. For the present case, this length is quite long (~ 50 Å), in semiquantitative accord with self-consistent calculations.[6,8] This is again a good limiting form for λ_i: the larger the gap (V_1), the more strongly damped the function. Using this simple procedure, we have generated a curve which should be proportional to I_s; this is shown, scaled to the maximum of our data, as the solid curve in Fig. 4. The fit to experiment is perhaps not as bad as might be implied by the figure. This is a zero-parameter fit, and the experimental results are at least qualitatively explained. Compared to the width of the Brillouin zone ($2k_L$), both curves are quite narrow.

Not surprisingly, the most sensitive parameter in determining the width calculated in Fig. 4 is V_1, which was fixed at the value determined by fitting Fermi-surface data.[21] Qualitatively, the smaller the value of V_1, the more the surface-state penetrates the bulk [Eq. (7)], and the more sharply peaked its Fourier spectrum. That the previous results for the $\bar{\Gamma}$ surface state on Al(001) (Ref. 4) are not as sharply peaked as they are here is because V_{200} is 4 times larger than V_{111} for aluminum. These results suggest a method for determining λ_i experimentally. Unfortunately, in order to force the calculation to fit our results, we need to set $V_1 \sim 0.8$ eV, a value which is unacceptably large.

An explanation for the misfit in Fig. 4 is suggested by the value of λ_i implied by this value of V_1. From Eq. (7), this is ~ 10 Å, which is close to typical values for the mean free path of 50-eV electrons in aluminum.[4,28,29] Apparently, the misfit is due to the fact that the decay length of the surface state is longer than the sampling depth of the ARPES probe. The fallacy in our model is in assuming strict $k_\perp$ conservation in Eq. (3). Broadening in $k_\perp$ in bulk direct transitions is a well-documented effect;[4,19,28] it should be included here to fit our results. We have convoluted a Lorentzian $k_\perp$ broadening into Eq. (4). The best fit, $\Delta k_\perp \approx 0.14$ Å^{-1}, is shown as the dashed line in Fig. 4. Values for the photoelectron inverse lifetime,

$$\Gamma_e = \left[\frac{dE}{dk}\right]\Delta k_\perp \approx 4.5 \text{ eV} ,$$

and the mean free path

$$\lambda_e = 1/\Delta k_\perp = 7 \text{ Å} ,$$

can be derived.[19,28] These are in good agreement with accepted values given elsewhere.[4,29]

Unfortunately, an accurate estimate of λ_i is impossible since the major contribution to the observed width in Fig. 4 is that of the momentum broadening. We can, however, provide a minimum value,

$$\lambda_i \gtrsim 20 \text{ Å} ,$$

in rough accord with self-consistent calculations. A value smaller than this would require unphysical results for Γ_e and λ_e. A more sophisticated, single-step treatment of our data might allow a more accurate assessment of the surface-state wave function.[30] As indicated elsewhere,[6–8] finite-thickness slab calculations of surface states will make accurate characterization of this state difficult. This long decay length has direct bearing on the surface state and/or surface resonance question addressed earlier. In our opinion, for a perfect crystal (see Sec. IV), this is a true surface state which is almost a surface resonance. A resonance, of course, would penetrate the bulk with an infinite decay length.

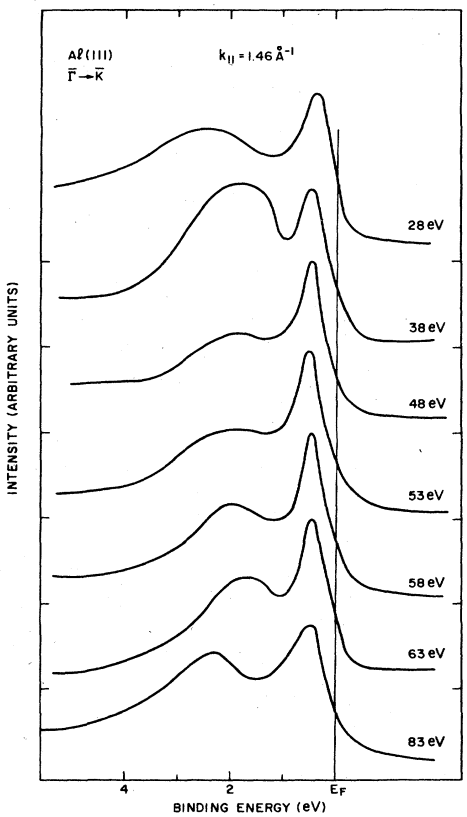

FIG. 5. Energy-distribution curves of Al(111) for various photon energies between 28 and 83 eV at the $\bar{K}$ point of the surface Brillouin zone. The peak near E_F is a surface state.

D. Results near $\bar{K}$

A final result on Al(111) is provided by the observation of another previously unobserved surface state at the $\bar{K}$ point of the two-dimensional Brillouin zone. Figure 5 shows several EDC's collected at $\bar{K}$ for $28 \leq h\nu \leq 83$ eV. The peak at $E_B = 0.7$ eV is seen not to disperse with $k_\perp$. In addition, the observed bulk transition at higher binding energy is clearly separated from the surface state at all energies, implying that the state is located entirely within a projected bulk gap and is hence a true surface state. The intensity of the surface state relative to that of the bulk is fairly independent of $\hbar\omega$ in this case, implying a rather localized state. This is in accord with the recent self-consistent calculations.[7,8] Our simple model will break down in this case; we have not attempted any semiquantitative treatments of these data.

Figure 6 shows EDC's of this state as a function of emission angle for parallel momenta near the $\bar{K}$-symmetry point. The state disperses upward across E_F rapidly, being observable only over a range of $\Delta k_{||} = 0.3$ Å^{-1}. Unfortunately, the substantial width (~ 0.4 eV) of this state, and its proximity to E_F, precludes an accurate determination of its dispersion relation. Its existence and location are in good qualitative agreement with calculation.[6–8] A second state predicted at higher binding energy at $\bar{K}$, however, is not observed in our spectra.

IV. SURFACE-STATE–ENERGY WIDTHS

A. Introductory discussion

There has recently been much interest in the various contributions to observed ARPES peak widths. All analyses start with contributions from the photohole and photoelectron lifetimes Γ_h and Γ_e.[11–13,19,28] At normal emission, the contribution of these lifetimes is[28]

$$\Gamma_0 = \left| \left| \frac{v_h}{v_e} \right| \Gamma_e + \Gamma_h \right| \Big/ \left| 1 - \frac{v_h}{v_e} \right| , \tag{10}$$

where Γ_0 is the observed lifetime width and v_h and v_e are the band velocities of the final-state hole and electron normal to the surface, respectively. For a surface state, $v_h = 0$ and $\Gamma_0 = \Gamma_h$. Recent high-resolution studies of copper surface states[11–13] have demonstrated the existence of a less fundamental, but, in some cases, equally important, broadening mechanism. Surface imperfections—defects and impurities—weaken the parallel-momentum–conservation condition in ARPES in such a way that the peak is further broadened:

$$\Gamma_1 = v_{||} \Delta k_{||} , \tag{11}$$

where $v_{||}$ is the initial band velocity parallel to the surface, and $\Delta k_{||}$ is a measure of the momentum broadening. The observed width is, in addition, affected by the experimental energy and momentum resolution. The latter of these can be absorbed into Γ_1 by endowing $\Delta k_{||}$ with experimental and fundamental contributions. All of these contributions must be convoluted to produce the observed width.[31] For illustrative purposes, we assume here that the contributions convolute as Lorentzians so that the widths simply add:

$$\Gamma = \Gamma_0 + v_{||} \Delta k_{||} + \Delta E_0 . \tag{12}$$

ΔE_0 for now is taken to be a measure of the experimental energy resolution. For a surface state near E_F, the contribution from Γ_0 is small, so that

$$\Gamma = v_{||} \Delta k_{||} + \Delta E_0 . \tag{13}$$

The systematic errors introduced by this deconvolution will not significantly affect our final conclusions.[31]

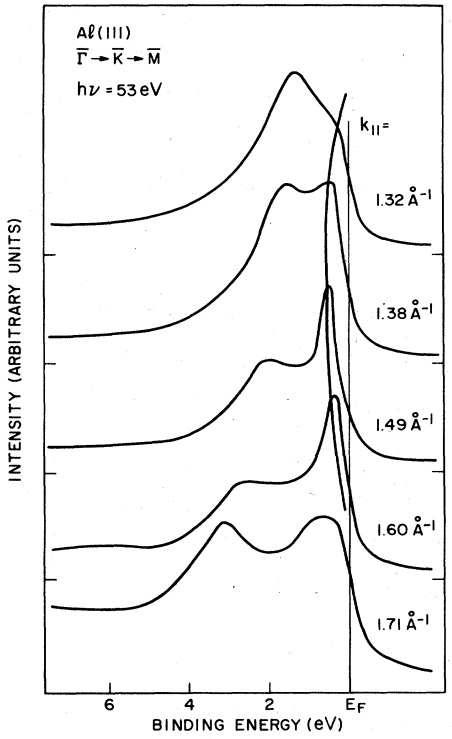

FIG. 6. Energy-distribution curves of Al(111) for various parallel momenta near the $\bar{K}$ point at $h\nu = 53$ eV.

B. Results on Al(001)

In an attempt to apply this formalism to aluminum, we have measured the widths of the $\bar{\Gamma}$ surface states on both surfaces as a function of $k_{||}$. The various spectra for Al(001) shown in Fig. 7 yield a parabolic dispersion relation[4] qualitatively similar to that observed on Cu(111).[11] The surface-state width is plotted in Fig. 8, where a slow increase is observed as $|k_{||}|$ increases. This reflects a contribution from the first term in Eq. (13), since $v_{||}$ increases away from $\bar{\Gamma}$. Proceeding as before,[11–13] the slope of this curve near E_F yields a value for the $\Delta k_{||} \sim 0.05$ Å^{-1} broadening. There is a small contribution (~ 0.01 Å^{-1}) to this result from the experimental momentum resolution, but the dominant contribution is due to the fundamental parallel-momentum broadening mentioned earlier. This value is reasonable in consideration of the values observed previously in copper[11–13] (0.02–0.04 Å^{-1}). The discussion below indicates that this estimate is quite rough in any case.

A further analysis of these results yields a contradiction. The contribution from the first term at the Fermi

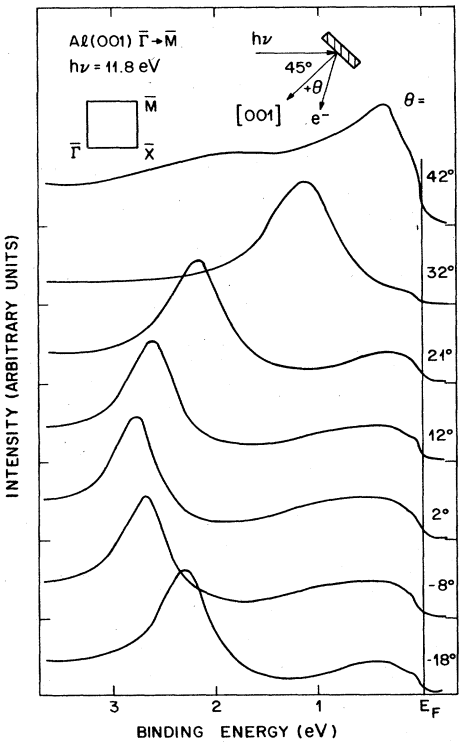

FIG. 7. Energy-distribution curves of the $\bar{\Gamma}$ surface state on Al(001) at $h\nu=11.85$ eV. Upward parabolic dispersion about the $\bar{\Gamma}$ point is observed.

level in Eq. (13) is just $v_F\Delta k_{||}\sim 0.35$ eV, yielding a value of 0.4 eV for ΔE_0 in Eq. (13). Our energy resolution has been measured to be only 40 meV under the conditions used, implying that there must be some other broadening

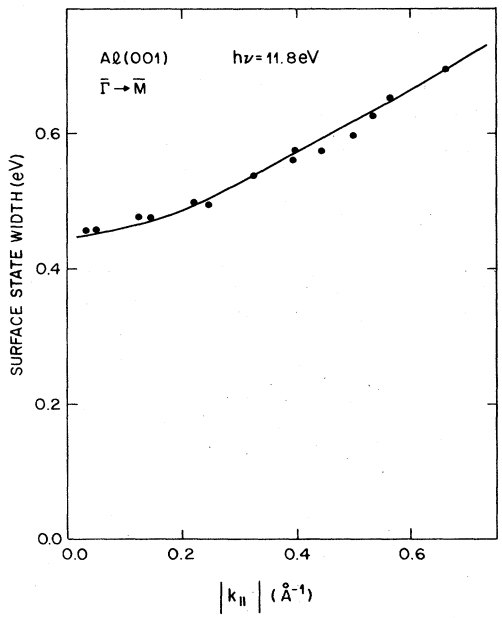

FIG. 8. Energy width of the $\bar{\Gamma}$ surface state on Al(001) as a function of $|k_{||}|$ in the $\bar{\Gamma}\rightarrow\bar{M}$ azimuth.

mechanism. A similar analysis for the surface state at $\bar{\Gamma}$ on Al(111) requires additional broadening of 1.5–2.0 eV. This clearly is beyond experimental error. There was no similar contradiction for the previous studies on copper.[11–13]

C. Additional broadening mechanism

A reexamination of the assumptions used so far is in order. Equation (10) is strictly valid only for normal emission. Using a more complex form given elsewhere[24] does not significantly alter the magnitude of the effect ($<20\%$). A more serious discussion of the assumptions used in Ref. 24 to derive Eq. (10) is necessary. The derivation has, in effect, been validated by applications to a variety of systems possessing s, p, and d bands which are more complex than aluminum.[11–13,19,28] There is no particular reason to expect aluminum to be a special case. The expansions which neglect terms of second and higher order apparently work well in other materials, and should also be adequate for aluminum. This is supported by the success in treating the energy widths of bulk features for Al(001).[4] The anomaly lies in the widths of the surface states alone.

A mechanism for this additional broadening can be proposed. It is tempting to conclude that these states are actually resonances which would be broadened essentially by an initial-state resonance lifetime.[11,22] For the case of Al(001), however, the splitting from the bulk continuum has been measured to be ~ 0.1 eV,[4] and the analysis of the preceding subsection supports the conclusion that the state on Al(111) is a true surface state as well. It is significant, however, that the splitting of the surface state from the bulk continuum on Al(111) is probably less than that on Al(001). In simple theories, this splitting scales with the magnitude of the potential matrix element creating the gap.[26,27] Hence, the surface state on Al(111) should be split by $\sim\frac{1}{4}$ the value of that on Al(001). Since the enhanced broadening is 4–5 times larger on Al(111) than on Al(001), it appears, qualitatively, that the broadening scales inversely with the splitting from the bulk continuum.

A clue to the source of the additional broadening is indicated in Fig. 3. The splitting of the surface-state dispersion from the bulk continuum is probably less than the inverse lifetime of the photohole on the energy axis, and is generally comparable to or less than the fundamental momentum broadening on the momentum axis. This implies that for an imperfect crystal—one with a hole in its valence band or with defects and impurities—these pure states become resonances. In other words, both the bulk-continuum edge and the surface-state dispersion relation become indistinct and, hence, overlap. This allows defect-assisted interactions between the two, and implies a finite resonance lifetime for electrons or holes in the surface-state band.

V. SUMMARY AND CONCLUSIONS

We have observed two new surface states on Al(111) at the $\bar{\Gamma}$ and $\bar{K}$ points. A simple model which explains the fact that the $\bar{\Gamma}$ surface state is observable over only a nar-

row range of photon energies was described. Further theoretical work might allow extraction of certain characteristics of the surface-state wave function if the effect of the final-state photoelectron mean free path can be adequately included. Finally, contradictions in the interpretation of the observed surface-state peak widths within the framework of current models have led to the hypothesis of a new and independent broadening mechanism.

ACKNOWLEDGMENTS

One of us (S.D.K.) is thankful to J. Tersoff for useful discussions. This work was done in part at the National Synchrotron Light Source at Brookhaven National Laboratory under the auspices of the Department of Energy, Contract No. DE-AC02-76-CH00016.

[1]D. S. Boudreaux, Surf. Sci. **28**, 344 (1971).
[2]P. O. Gartland and B. J. Slagsvold, Solid State Commun. **25**, 489 (1978).
[3]G. V. Hansson and S. A. Flödstrom, Phys. Rev. B **18**, 1562 (1978).
[4]H. J. Levinson, F. Greuter, and E. W. Plummer, Phys. Rev. B **27**, 727 (1983).
[5]J. K. Grepstad and B. J. Slagsvold, Phys. Scr. **25**, 813 (1982).
[6]J. R. Chelikowski, M. Schlüter, S. G. Louie, and M. L. Cohen, Solid State Commun. **17**, 1103 (1975).
[7]D. Wang, A. J. Freeman, H. Krakauer, and M. Posternak, Phys. Rev. B **23**, 1685 (1981).
[8]K. Mednick and L. Kleinman, Phys. Rev. B **22**, 5768 (1980).
[9]D. Spanjaard, D. W. Jepsen, and P. M. Marcus, Phys. Rev. B **19**, 642 (1979).
[10]S. G. Louie, P. Thiry, R. Pinchaux, Y. Petroff, D. Chandesris, and J. Lecante, Phys. Rev. Lett. **44**, 549 (1980).
[11]S. D. Kevan, Phys. Rev. Lett. **50**, 526 (1983).
[12]J. Tersoff and S. D. Kevan, Phys. Rev. B **28**, 4267 (1983).
[13]S. D. Kevan, Phys. Rev. B **28**, 4822 (1983).
[14]S. D. Kevan, Rev. Sci. Instrum. **54**, 1441 (1983).
[15]P. Thiry, P. A. Bennett, S. D. Kevan, W. A. Royer, E. E. Chaban, J. E. Rowe, and N. V. Smith, Nucl. Instrum. Methods **222**, 85 (1984).
[16]E. W. Plummer and W. Eberhardt, *Advances in Chemical Physics* (Wiley, New York, 1982), Vol. 49, p. 533.
[17]R. F. Willis and B. Feuerbacher, in *Photoemission and the Electronic Properties of Surfaces*, edited by B. Feuerbacher, B. Fritton, and R. F. Willis (Wiley, New York, 1978).
[18]K. Forstmann, in Ref. 17.
[19]P. Thiry, D. Chandesris, J. Lacante, C. Guillot, R. Pinchaux, and Y. Petroff, Phys. Rev. Lett. **43**, 82 (1979).
[20]We have adopted the free-electron-like final-state bands derived in Ref. 4, using $V_0 = -11.6$ eV and $m^* = m_e$.
[21]J. R. Anderson and S. S. Lane, Phys. Rev. B **2**, 298 (1970).
[22]R. A. DiDio, E. W. Plummer, and W. R. Graham, Phys. Rev. Lett. **52**, 683 (1984).
[23]S. A. Kevan, N. G. Stoffel, and N. V. Smith (unpublished).
[24]P. Thiry, Ph.D. thesis, Université Paris Sud, 1981.
[25]Y. Petroff and P. Thiry, Appl. Opt. **19**, 3957 (1980).
[26]*Solid State Physics*, edited by N. W. Ashcroft and N. D. Mermin (Holt, Rinehardt and Winston, New York, 1976).
[27]E. T. Goodwin, Proc. Cambridge Philos. Soc. **35**, 205 (1939).
[28]J. A. Knapp, F. J. Himpsel, and D. E. Eastman, Phys. Rev. B **19**, 4952 (1979).
[29]W. E. Spicer, J. Phys. (Paris) Colloq. **34**, C6-19 (1973).
[30]J. B. Pendry and J. F. L. Hopkinson, J. Phys. (Paris) Colloq. **39**, C4-142 (1978).
[31]Appendix II of Ref. 24 presents a complete analysis of the experimental and lifetime contributions to observed peak widths for arbitrary band dispersions and emission angles. Significant simplifications occur for the simple systems presented here, and our ultimate conclusions are unaffected by our simplified analysis.